



# TECH BRIEFS

NATIONAL AERONAUTICS AND SPACE ADMINISTRATION

-  **Technology Focus**
-  **Electronics/Computers**
-  **Software**
-  **Materials**
-  **Mechanics/Machinery**
-  **Manufacturing**
-  **Bio-Medical**
-  **Physical Sciences**
-  **Information Sciences**
-  **Books and Reports**



## INTRODUCTION

Tech Briefs are short announcements of innovations originating from research and development activities of the National Aeronautics and Space Administration. They emphasize information considered likely to be transferable across industrial, regional, or disciplinary lines and are issued to encourage commercial application.

### Additional Information on NASA Tech Briefs and TSPs

Additional information announced herein may be obtained from the NASA Technical Reports Server: <http://ntrs.nasa.gov>.

Please reference the control numbers appearing at the end of each Tech Brief. Information on NASA's Innovative Partnerships Program (IPP), its documents, and services is available on the World Wide Web at <http://www.ipp.nasa.gov>.

Innovative Partnerships Offices are located at NASA field centers to provide technology-transfer access to industrial users. Inquiries can be made by contacting NASA field centers listed below.

## NASA Field Centers and Program Offices

### Ames Research Center

David Morse  
(650) 604-4724  
[david.r.morse@nasa.gov](mailto:david.r.morse@nasa.gov)

### Dryden Flight Research Center

Ron Young  
(661) 276-3741  
[ronald.m.young@nasa.gov](mailto:ronald.m.young@nasa.gov)

### Glenn Research Center

Kimberly A. Dalgleish-Miller  
(216) 433-8047  
[kimberly.a.dalgleish@nasa.gov](mailto:kimberly.a.dalgleish@nasa.gov)

### Goddard Space Flight Center

Nona Cheeks  
(301) 286-5810  
[nona.k.cheeks@nasa.gov](mailto:nona.k.cheeks@nasa.gov)

### Jet Propulsion Laboratory

Indrani Graczyk  
(818) 354-2241  
[indrani.graczyk@jpl.nasa.gov](mailto:indrani.graczyk@jpl.nasa.gov)

### Johnson Space Center

John E. James  
(281) 483-3809  
[john.e.james@nasa.gov](mailto:john.e.james@nasa.gov)

### Kennedy Space Center

David R. Makufka  
(321) 867-6227  
[david.r.makufka@nasa.gov](mailto:david.r.makufka@nasa.gov)

### Langley Research Center

Michelle Ferebee  
(757) 864-5617  
[michelle.t.ferebee@nasa.gov](mailto:michelle.t.ferebee@nasa.gov)

### Marshall Space Flight Center

Terry L. Taylor  
(256) 544-5916  
[terry.taylor@nasa.gov](mailto:terry.taylor@nasa.gov)

### Stennis Space Center

Ramona Travis  
(228) 688-3832  
[ramona.e.travis@ssc.nasa.gov](mailto:ramona.e.travis@ssc.nasa.gov)

### NASA Headquarters

Daniel Lockney,  
Technology Transfer Program Executive  
(202) 358-2037  
[daniel.p.lockney@nasa.gov](mailto:daniel.p.lockney@nasa.gov)

### Small Business Innovation Research (SBIR) & Small Business Technology Transfer (STTR) Programs

Rich Leshner, Program Executive  
(202) 358-4920  
[rleshner@nasa.gov](mailto:rleshner@nasa.gov)





# TECH BRIEFS

NATIONAL AERONAUTICS AND SPACE ADMINISTRATION



## 5 Technology Focus: Data Acquisition

- 5 Visual System for Browsing, Analysis, and Retrieval of Data (ViSBARD)
- 5 Time-Domain Terahertz Computed Axial Tomography NDE System
- 6 Adaptive Sampling of Time Series During Remote Exploration
- 6 A Tracking Sun Photometer Without Moving Parts
- 7 Surface Temperature Data Analysis
- 7 Modular, Autonomous Command and Data Handling Software With Built-In Simulation and Test
- 8 *In-Situ* Wire Damage Detection System



## 9 Electronics/Computers

- 9 Amplifier Module for 260-GHz Band Using Quartz Waveguide Transitions
- 9 Wideband Agile Digital Microwave Radiometer



## 11 Manufacturing & Prototyping

- 11 FACT, Mega-ROSA, SOLAROSA



## 13 Materials & Coatings

- 13 An Integrated, Layered-Spinel Composite Cathode for Energy Storage Applications
- 13 Engineered Multifunctional Surfaces for Fluid Handling
- 14 Polyolefin-Based Aerogels
- 15 Adjusting Permittivity by Blending Varying Ratios of SWNTs



## 17 Mechanics/Machinery

- 17 Gravity-Assist Mechanical Simulator for Outreach
- 17 Concept for Hydrogen-Impregnated Nanofiber/Photovoltaic Cargo Stowage System
- 18 DROP: Durable Reconnaissance and Observation Platform



## 21 Bio-Medical

- 21 Developing Physiologic Models for Emergency Medical Procedures Under Microgravity



## 23 Physical Sciences

- 23 Spectroscopic Chemical Analysis Methods and Apparatus
- 23 Low Average Sidelobe Slot Array Antennas for Radiometer Applications
- 24 Motion-Corrected 3D Sonic Anemometer for Tethersondes and Other Moving Platforms
- 24 Water Treatment Systems for Long Spaceflights
- 25 Microchip Non-Aqueous Capillary Electrophoresis ( $\mu$ NACE) Method to Analyze Long-Chain Primary Amines
- 25 Low-Cost Phased Array Antenna for Sounding Rockets, Missiles, and Expendable Launch Vehicles
- 26 Mars Science Laboratory Engineering Cameras
- 26 Seismic Imager Space Telescope



## 29 Information Technology

- 29 Estimating Sea Surface Salinity and Wind Using Combined Passive and Active L-Band Microwave Observations
- 29 A Posteriori Study of a DNS Database Describing Supercritical Binary-Species Mixing
- 30 Scalable SCPPM Decoder



## 31 Software

- 31 QuakeSim 2.0
- 31 HURON (HUMAN and Robotic Optimization Network) Multi-Agent Temporal Activity Planner/Scheduler
- 31 MPST Software: MoonKommand

This document was prepared under the sponsorship of the National Aeronautics and Space Administration. Neither the United States Government nor any person acting on behalf of the United States Government assumes any liability resulting from the use of the information contained in this document, or warrants that such use will be free from privately owned rights.





## Visual System for Browsing, Analysis, and Retrieval of Data (ViSBARD)

*Goddard Space Flight Center, Greenbelt, Maryland*

ViSBARD software provides a way of visualizing multiple vector and scalar quantities as measured by many spacecraft at once. The data are displayed three-dimensionally along the orbits that may be shown either as connected lines or as points. The data display allows the rapid determination of vector configurations, correlations among many measurements at multiple points, and global relationships. Things such as vector field rotations and dozens of simultaneous variables are very difficult to see in (complementary) panel plot representations.

The current and next generations of space physics missions require a means to display from tens to hundreds of time series of data in such a way that the mind can comprehend them for the purposes of browsing data, retrieving them in directly useful form, and analyzing them in a global context. Sets of many spacecraft, each carrying many instruments yielding nearly continuous data at high time resolution, have become one of the most effective ways to make progress in understanding the extended, ionized (plasma) atmosphere of the Earth and the Sun. For large collections of data to be effective,

they must be extremely readily accessible, with simple, comprehensible overviews of what is available. ViSBARD provides a means to answer these concerns.

The ViSBARD package also acts as a remote repository browser; an interface to a Virtual Observatory. Therefore, data can be pulled directly into the application, as opposed to searching for it and downloading separately.

*This work was done by Aaron Roberts and Ryan Boller of Goddard Space Flight Center, and Carl Cornwell of Aquilent, Inc. Further information is contained in a TSP (see page 1). GSC-15744-1*

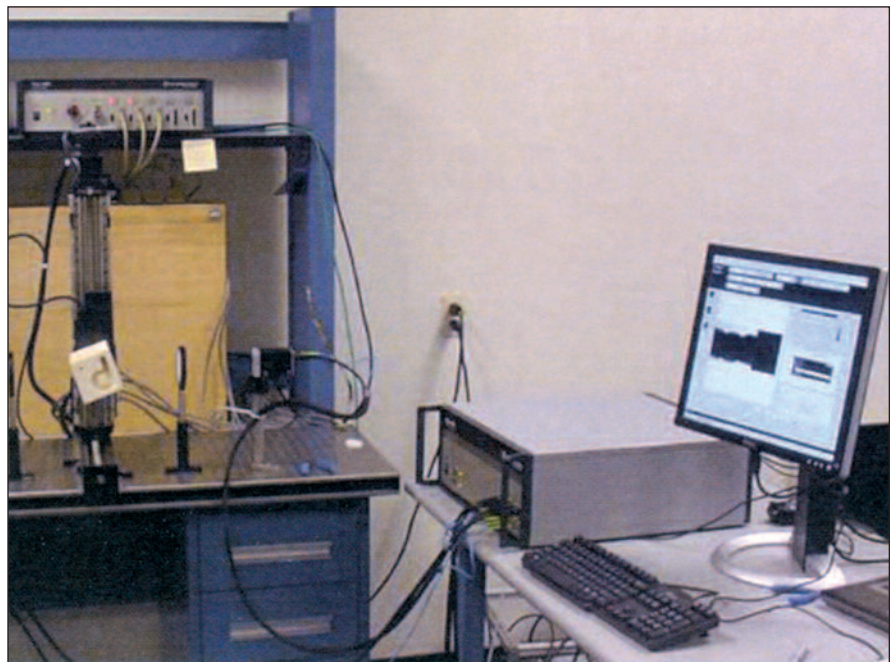
## Time-Domain Terahertz Computed Axial Tomography NDE System

**3D terahertz tomography can characterize aging, durability, and flaw conditions in materials for thermal protection systems and composite overwrap pressure vessels.**

*John H. Glenn Research Center, Cleveland, Ohio*

NASA has identified the need for advanced non-destructive evaluation (NDE) methods to characterize aging and durability in aircraft materials to improve the safety of the nation's airline fleet. 3D THz tomography can play a major role in detection and characterization of flaws and degradation in aircraft materials, including Kevlar-based composites and Kevlar and Zylon fabric covers for soft-shell fan containment where aging and durability issues are critical.

A prototype computed tomography (CT) time-domain (TD) THz imaging system has been used to generate 3D images of several test objects including a TUFU tile (a thermal protection system tile used on the Space Shuttle and possibly the Orion or similar capsules). This TUFU tile had simulated impact damage that was located and the depth of damage determined. The CT motion control gantry was designed and constructed, and then integrated with a T-Ray 4000<sup>®</sup> control unit



The CT TD-THz System testbed with the gantry (left) and TD-THz control unit (right).

and motion controller to create a complete CT TD-THz imaging system prototype. A data collection software script was developed that takes multiple z-axis slices in sequence and saves the data for batch processing. The data collection software was integrated with the ability to batch process the slice data with the CT TD-THz image reconstruction software. The time required to take a single CT slice was decreased from six minutes to approximately one minute by replacing the 320 ps, 100-Hz waveform acquisition system with an 80 ps, 1,000-Hz waveform acquisition system.

The TD-THz computed tomography system was built from pre-existing commercial off-the-shelf subsystems. A CT motion control gantry was constructed from COTS components that can handle larger samples. The motion control gantry allows inspection of sample sizes of up to approximately one cubic foot ( $\approx 0.03 \text{ m}^3$ ). The system reduced to practice a CT-TD-THz system incorporating a COTS 80-ps/1-kHz waveform scanner. The incorporation of this scanner in the system allows acquisition of 3D slice data with better signal-to-noise using a COTS scanner rather than the “chirped” scanner. The system also reduced to practice a prototype for

commercial CT systems for insulating materials where safety concerns cannot accommodate x-ray. A software script was written to automate the COTS software to collect and process TD-THz CT data.

*This work was done by David Zimdars of Picometrix LLC, subsidiary of Advanced Photonix, Inc. (Amex: API) for Glenn Research Center. Further information is contained in a TSP (see page 1).*

*Inquiries concerning rights for the commercial use of this invention should be addressed to NASA Glenn Research Center, Innovative Partnerships Office, Attn: Steven Fedor, Mail Stop 4-8, 21000 Brookpark Road, Cleveland, Ohio 44135. Refer to LEW-18776-1.*

---

## Adaptive Sampling of Time Series During Remote Exploration

The challenge is addressed as an “active learning” problem.

*NASA's Jet Propulsion Laboratory, Pasadena, California*

This work deals with the challenge of online adaptive data collection in a time series. A remote sensor or explorer agent adapts its rate of data collection in order to track anomalous events while obeying constraints on time and power. This problem is challenging because the agent has limited visibility (all its datapoints lie in the past) and limited control (it can only decide when to collect its next datapoint). This problem is treated from an information-theoretic perspective, fitting a probabilistic model to collected data and optimizing the future sampling strategy to maximize information gain. The performance characteristics of stationary and nonstationary Gaussian process models are compared.

Self-throttling sensors could benefit environmental sensor networks and monitoring as well as robotic exploration. Explorer agents can improve performance by adjusting their data collec-

tion rate, preserving scarce power or bandwidth resources during uninteresting times while fully covering anomalous events of interest. For example, a remote earthquake sensor could conserve power by limiting its measurements during normal conditions and increasing its cadence during rare earthquake events. A similar capability could improve sensor platforms traversing a fixed trajectory, such as an exploration rover transect or a deep space flyby. These agents can adapt observation times to improve sample coverage during moments of rapid change.

An adaptive sampling approach couples sensor autonomy, instrument interpretation, and sampling. The challenge is addressed as an “active learning” problem, which already has extensive theoretical treatment in the statistics and machine learning literature. A statistical Gaussian process (GP) model is em-

ployed to guide sample decisions that maximize information gain. Nonstationary (e.g., time-varying) covariance relationships permit the system to represent and track local anomalies, in contrast with current GP approaches.

Most common GP models are “stationary,” e.g., the covariance relationships are time-invariant. In such cases, information gain is independent of previously collected data, and the optimal solution can always be computed in advance. Information-optimal sampling of a stationary GP time series thus reduces to even spacing, and such models are not appropriate for tracking localized anomalies. Additionally, GP model inference can be computationally expensive.

*This work was done by David R. Thompson of Caltech for NASA's Jet Propulsion Laboratory. For more information, contact iaofice@jpl.nasa.gov. NPO-48430*

---

## A Tracking Sun Photometer Without Moving Parts

This reliable instrument is used to collect valuable information about the atmosphere.

*Ames Research Center, Moffett Field, California*

This innovation is small, lightweight, and consumes very little electricity as it measures the solar energy attenuated by gases and aerosol particles in the atmosphere. A Sun photometer is commonly used on the Earth's surface, as well as on aircraft, to determine the

solar energy attenuated by aerosol particles in the atmosphere and their distribution of sizes. This information is used to determine the spatial and temporal distribution of gases and aerosols in the atmosphere, as well as their distribution sizes.

The design for this Sun photometer uses a combination of unique optics and a charge coupled device (CCD) array to eliminate moving parts and make the instrument more reliable. It could be self-calibrating throughout the year. Data products would be down-welling flux,

the direct-diffuse flux ratio, column abundance of gas phase constituents, aerosol optical depth at multiple-wavelengths, phase functions, cloud statistics, and an estimate of the representative size of atmospheric particles. These measurements can be used to obtain an estimate of aerosol size distribution, refractive index, and particle shape.

Incident light is received at a light-reflecting (inner) surface, which is a truncated paraboloid. Light arriving from a hemispheric field of view (solid angle  $2\pi$  steradians) enters the reflecting optic at

an entrance aperture at, or adjacent to, the focus of the paraboloid, and is captured by the optic. Most of this light is reflected from an inner surface. The light proceeds substantially parallel to the paraboloid axis, and is detected by an array detector located near an exit aperture. Each of the entrance and exit apertures is formed by the intersection of the paraboloid with a plane substantially perpendicular to the paraboloid axis. Incident (non-reflected) light from a source of limited extent (the Sun) illuminates a limited area on the detector array. Both

direct and diffuse illumination may be reflected, or not reflected, before being received on the detector array. As the Sun traverses a path in the sky over some time interval, the track of the Sun can be traced on the detector array.

A suitably modified Sun photometer might be used to study the dynamics of an environment on another planet or satellite with an atmosphere.

*This work was done by Anthony W. Strawa of Ames Research Center. Further information is contained in a TSP (see page 1). ARC-15443-1*

---

## Surface Temperature Data Analysis

*Goddard Space Flight Center, Greenbelt, Maryland*

Small global mean temperature changes may have significant to disastrous consequences for the Earth's climate if they persist for an extended period. Obtaining global means from local weather reports is hampered by the uneven spatial distribution of the reliably reporting weather stations. Methods had to be developed that minimize as far as possible the impact of that situation.

This software is a method of combining temperature data of individual stations to obtain a global mean trend, overcoming/estimating the uncertainty introduced by the spatial and temporal gaps in the available data. Useful estimates were obtained by the introduction of a special grid, subdividing the Earth's surface into 8,000 equal-area boxes, using the existing data to create

virtual stations at the center of each of these boxes, and combining temperature anomalies (after assessing the radius of high correlation) rather than temperatures.

*This work was done by James Hansen and Reto Ruedy of Goddard Space Flight Center. For further information, contact the Goddard Innovative Partnerships Office at (301) 286-5810. GSC-16243-1*

---

## Modular, Autonomous Command and Data Handling Software With Built-In Simulation and Test

**Commercial markets include telecommunications, remote sensing, and GIS imagers.**

*Goddard Space Flight Center, Greenbelt, Maryland*

The spacecraft system that plays the greatest role throughout the program lifecycle is the Command and Data Handling System (C&DH), along with the associated algorithms and software. The C&DH takes on this role as cost driver because it is the brains of the spacecraft and is the element of the system that is primarily responsible for the integration and interoperability of all spacecraft subsystems. During design and development, many activities associated with mission design, system engineering, and subsystem development result in products that are directly supported by the C&DH, such as interfaces, algorithms, flight software (FSW), and parameter sets.

A modular system architecture has been developed that provides a means for rapid spacecraft assembly, test, and integration. This modular C&DH soft-

ware architecture, which can be targeted and adapted to a wide variety of spacecraft architectures, payloads, and mission requirements, eliminates the current practice of rewriting the spacecraft software and test environment for every mission. This software allows mission-specific software and algorithms to be rapidly integrated and tested, significantly decreasing time involved in the software development cycle.

Additionally, the FSW includes an On-board Dynamic Simulation System (ODySSy) that allows the C&DH software to support rapid integration and test. With this solution, the C&DH software capabilities will encompass all phases of the spacecraft lifecycle. ODySSy is an on-board simulation capability built directly into the FSW that provides dynamic built-in test capabilities as soon as the FSW image is loaded

onto the processor. It includes a six-degrees-of-freedom, high-fidelity simulation that allows complete closed-loop and hardware-in-the-loop testing of a spacecraft in a ground processing environment without any additional external stimuli. ODySSy can intercept and modify sensor inputs using mathematical sensor models, and can intercept and respond to actuator commands.

ODySSy integration is unique in that it allows testing of actual mission sequences on the flight vehicle while the spacecraft is in various stages of assembly, test, and launch operations — all without any external support equipment or simulators. The ODySSy component of the FSW significantly decreases the time required for integration and test by providing an automated, standardized, and modular approach to integrated avionics and com-

ponent interface and functional verification. ODySSy further provides the capability for on-orbit support in the form of autonomous mission planning and fault protection.

Modular C&DH FSW based on the architecture described in this tech brief

was successfully demonstrated on-orbit as part of the United States Air Force Academy's FalconSat-5 technology demonstrator spacecraft, which launched in November of 2011. This flight program clearly demonstrated the benefits of the modular FSW approach, including built-

in test via ODySSy, throughout the lifecycle of the FalconSat-5 spacecraft.

*This work was led by John Cuseo of Advanced Solutions, Inc. for Goddard Space Flight Center. Further information is contained in a TSP (see page 1). GSC-16054-1*

---

## In-Situ Wire Damage Detection System

*John F. Kennedy Space Center, Florida*

An In-Situ Wire Damage Detection System (ISWDDS) has been developed that is capable of detecting damage to a wire insulation, or a wire conductor, or to both. The system will allow for real-time, continuous monitoring of wiring health/integrity and reduce the number of false negatives and false positives while being smaller, lighter in weight, and more robust than current systems. The technology allows for improved safety and significant reduction in maintenance hours for aircraft, space vehicles, satellites, and other critical high-performance wiring systems for industries such as energy production and mining.

The integrated ISWDDS is comprised of two main components: (1) a wire with

an innermost core conductor, an inner insulation film, a conductive layer or inherently conductive polymer (ICP) covering the inner insulation film, an outermost insulation jacket; and (2) smart connectors and electronics capable of producing and detecting electronic signals, and a central processing unit (CPU) for data collection and analysis. The wire is constructed by applying the inner insulation films to the conductor, followed by the outer insulation jacket. The conductive layer or ICP is on the outer surface of the inner insulation film. One or more wires are connected to the CPU using the smart connectors, and up to 64 wires can be monitored in real-time.

The ISWDDS uses time domain reflectometry for damage detection. A

fast-risetime pulse is injected into either the core conductor or conductive layer and referenced against the other conductor, producing transmission line behavior. If either conductor is damaged, then the signal is reflected. By knowing the speed of propagation of the pulse, and the time it takes to reflect, one can calculate the distance to and location of the damage.

*This work was done by Martha Williams, Luke Roberson, Lanetra Tate, and Trent Smith of Kennedy Space Center; and Tracy Gibson, Pedro Medelius, and Scott Jolley of ASRC Aerospace Corporation. For more information, contact the Kennedy Space Center Innovative Partnerships Office at 321-867-5033. KSC-12866*



## Amplifier Module for 260-GHz Band Using Quartz Waveguide Transitions

**The development of high-performance, low-noise amplifiers has applications for future earth science and planetary instruments with low power and volume.**

*NASA's Jet Propulsion Laboratory, Pasadena, California*

Packaging of MMIC LNA (monolithic microwave integrated circuit low-noise amplifier) chips at frequencies over 200 GHz has always been problematic due to the high loss in the transition between the MMIC chip and the waveguide medium in which the chip will typically be used. In addition, above 200 GHz, wire-bond inductance between the LNA and the waveguide can severely limit the RF matching and bandwidth of the final waveguide amplifier module.

This work resulted in the development of a low-loss quartz waveguide transition that includes a capacitive transmission line between the MMIC and the waveguide probe element. This capacitive transmission line tunes out the wire-bond inductance (where the wire-bond is required to bond between the MMIC and the probe element). This inductance can severely limit the RF matching and bandwidth of the final waveguide amplifier module.

The amplifier module consists of a quartz E-plane waveguide probe transition, a short capacitive tuning element, a short wire-bond to the MMIC, and the MMIC LNA. The output structure is similar, with a short wire-bond at the output of the MMIC, a quartz E-plane waveguide probe transition, and the output waveguide. The quartz probe element is made of 3-mil quartz, which is the thinnest commercially available material. The waveguide band used is WR4, from 170 to 260 GHz. This new transition and block design is an improvement over prior art because it provides for better RF matching, and will likely yield lower loss and better noise figure.

The development of high-performance, low-noise amplifiers in the 180-to-700-GHz range has applications for future earth science and planetary instruments with low power and volume, and astrophysics array instruments for molecular spectroscopy.

This frequency band, while suitable for homeland security and commercial applications (such as millimeter-wave imaging, hidden weapons detection, crowd scanning, airport security, and communications), also has applications for future NASA missions. The Global Atmospheric Composition Mission (GACM) in the NRC Decadal Survey will need low-noise amplifiers with extremely low noise temperatures, either at room temperature or for cryogenic applications, for atmospheric remote sensing.

*This work was done by Sharmila Padmanabhan, King Man Fung, Pekka P. Kangaslahti, Alejandro Peralta, Mary M. Soria, David M. Pukala, Seth Sim, and Lorene A. Samoska of Caltech; and Stephen Sarkozy and Richard Lai of Northrop Grumman Corporation for NASA's Jet Propulsion Laboratory. Further information is contained in a TSP (see page 1). NPO-48436*

## Wideband Agile Digital Microwave Radiometer

**This technology can be applied to terrestrial science instruments.**

*NASA's Jet Propulsion Laboratory, Pasadena, California*

The objectives of this work were to take the initial steps needed to develop a field programmable gate array (FPGA)-based wideband digital radiometer backend (>500 MHz bandwidth) that will enable passive microwave observations with minimal performance degradation in a radio-frequency-interference (RFI)-rich environment. As manmade RF emissions increase over time and fill more of the microwave spectrum, microwave radiometer science applications will be increasingly impacted in a negative way, and the current generation of spaceborne microwave radiometers that use broadband analog back ends

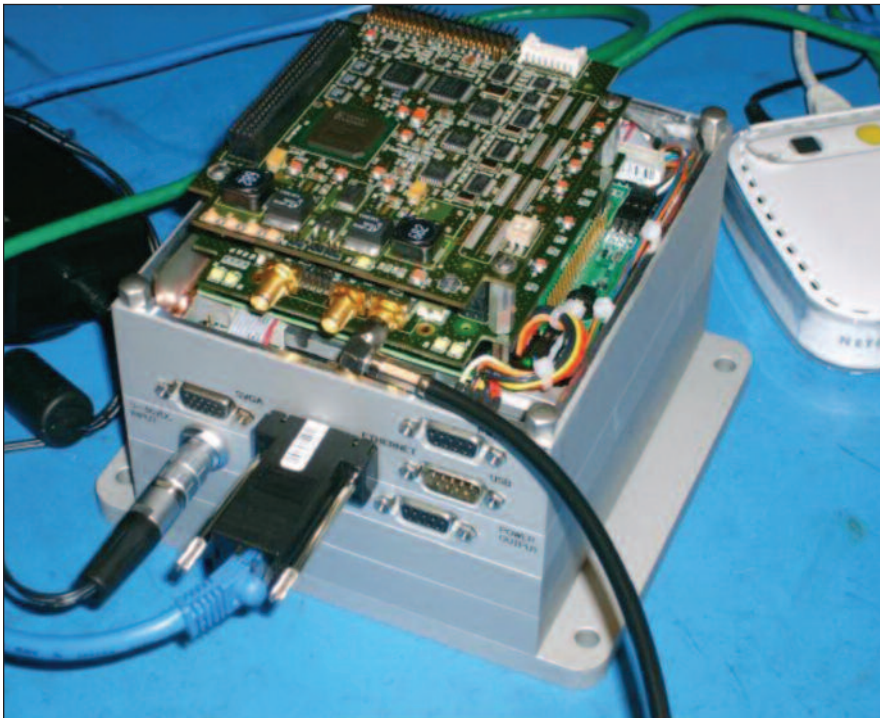
will become severely compromised or unusable over an increasing fraction of time on orbit.

There is a need to develop a digital radiometer back end that, for each observation period, uses digital signal processing (DSP) algorithms to identify the maximum amount of RFI-free spectrum across the radiometer band to preserve bandwidth to minimize radiometer noise (which is inversely related to the bandwidth).

Ultimately, the objective is to incorporate all processing necessary in the back end to take contaminated input spectra and produce a single output value free of manmade signals to minimize data

rates for spaceborne radiometer missions. But, to meet these objectives, several intermediate processing algorithms had to be developed, and their performance characterized relative to typical brightness temperature accuracy requirements for current and future microwave radiometer missions, including those for measuring salinity, soil moisture, and snow pack.

Digital radiometer back ends with similar capabilities currently exist based on older FPGA technology with significantly narrower input bandwidths (10s of MHz). Wider bandwidths are now possible that will allow these back ends to meet the requirements of a much



The FPGA Wideband Digital Radiometer.

broader range of radiometer applications and future missions.

The approach was to design DSP modules for implementation using a commercial FPGA evaluation board with an integrated dual-channel analog-

to-digital converter (ADC), high-speed interfaced FPGA, and high-data-rate embedded computer interface. The board was packaged with a PC104 embedded computer running a real-time O/S for data analysis, packetization,

and storage. The complete system was programmed with appropriate firmware and software to function as an agile digital radiometer back end, capable of spectral sub-banding, kurtosis detection, RFI mitigation, and fully polarimetric complex correlation. It should be noted that this functionality duplicates and exceeds that of the existing Soil Moisture Active Passive brassboard digital back end, but with a factor of ~40 higher bandwidth.

This work advances the state-of-the-art in digital radiometer back ends by improving the system bandwidth by over an order of magnitude compared to other existing systems. It also makes possible the potential to include RFI mitigation onboard, which is critical for wide-bandwidth, multi-channel systems.

(At the time of this reporting, the SMAP mission has not been formally approved by NASA. The decision to proceed with the mission will not occur until the completion of the National Environmental Policy Act (NEPA) process. Material in this document related to SMAP is for information purposes only.)

*This work was done by Todd C. Gaier and Shannon T. Brown of Caltech, and Christopher Ruf and Steven Gross of the University of Michigan for NASA's Jet Propulsion Laboratory. Further information is contained in a TSP (see page 1). NPO-48287*



## Buckyball Nucleation of HiPco Tubes

*Lyndon B. Johnson Space Center, Houston, Texas*

The purpose of this innovation is to enhance nucleation of single-wall nanotubes (SWNTs) in the HiPco process, selectively producing 10,10 tubes, something which until now has not been thought possible.

This is accomplished by injecting  $C_{60}$ , or a derivative of  $C_{60}$ , solubilized in supercritical  $CO_2$  together with a transition metal carbonyl co-catalyst into the HiPco reactor. This is a variant on the "supercritical" disclosure.  $C_{60}$  has never

been used to nucleate carbon nanotubes in the gas phase.

$C_{60}$  itself may not have adequate solubility in supercritical  $CO_2$ . However, fluorinated  $C_{60}$ , e.g.,  $C_{60}F_{36}$ , is easy to make cheaply and should have much enhanced solubility.

*This work was done by Richard E. Smalley of Rice University for Johnson Space Center. For further information, contact the JSC Innovation Partnerships Office at (281) 483-3809.*

*In accordance with Public Law 96-517, the contractor has elected to retain title to this invention. Inquiries concerning rights for its commercial use should be addressed to:*

*Rice University*

*Office of Technology Transfer – MS 705*

*P.O. Box 1892*

*Houston, TX 77251-1892*

*Phone No. (713) 737-6143*

*Refer to MSC-24134-1, volume and number of this NASA Tech Briefs issue, and the page number.*

## FACT, Mega-ROSA, SOLAROSA

**These technologies have applications in fixed and mobile large-area photovoltaic renewable energy systems.**

*John H. Glenn Research Center, Cleveland, Ohio*

The Flexible Array Concentrator Technology (FACT) is a lightweight, high-performance reflective concentrator blanket assembly that can be used on flexible solar array blankets. The FACT concentrator replaces every other row of solar cells on a solar array blanket, significantly reducing the cost of the array. The modular design is highly scalable for the array system designer, and exhibits compact stowage, good off-pointing acceptance, and mass/cost savings. The assembly's relatively low concentration ratio, accompanied by a large radiative area, provides for a low cell operating temperature, and eliminates many of the thermal problems inherent in high-concentration-ratio designs. Unlike other reflector technologies, the FACT concentrator modules function on both z-fold and rolled flexible solar array blankets, as well as rigid array systems.

Mega-ROSA (Mega Roll-Out Solar Array) is a new, highly modularized and extremely scalable version of ROSA that provides immense power level range capability from 100 kW to several MW in size. Mega-ROSA will enable extremely high-power spacecraft and SEP-powered missions, including space-tug and large-scale planetary science and lunar/asteroid exploration missions. Mega-ROSA's

inherent broad power scalability is achieved while retaining ROSA's solar array performance metrics and mission-enabling features for lightweight, compact stowage volume and affordability.

This innovation will enable future ultra-high-power missions through low-cost (25 to 50% cost savings, depending on PV and blanket technology), lightweight, high specific power (>200 to 400 W/kg BOL (beginning-of-life) at the wing level depending on PV and blanket technology), compact stowage volume (>50 kW/m<sup>3</sup> for very large arrays), high reliability, platform simplicity (low failure modes), high deployed strength/stiffness when scaled to huge sizes, and high-voltage operation capability. Mega-ROSA is adaptable to all photovoltaic and concentrator flexible blanket technologies, and can readily accommodate standard multi-junction and emerging ultra-lightweight IMM (inverted metamorphic) photovoltaic flexible blanket assemblies, as well as ENTECH's Stretched Lens Array (SLA) and DSSs (Deployable Space Systems') FACT, which allows for cost reduction at the array level.

The SOLAROSA technology embodiment is the fusion of a mass-optimized ROSA structural system integrated to a new version of ENTECH's lightweight

SLA (Stretched Lens Array) linear refractive concentrator blanket assembly. The SOLAROSA flexible blanket concentrator solar array can be rolled or z-folded, and enables NASA's emerging Space Science and Exploration high-voltage solar electric propulsion (SEP) missions.

This innovation is a potentially revolutionary solar array that provides game-changing performance in terms of high specific power (>400 to 500 W/kg BOL at wing level), affordability (>50% projected cost savings at the array level), light weight, high deployed stiffness, high deployed strength, compact stowage volume (>60 to 80 kW/m<sup>3</sup> BOL), reliability, high radiation tolerance, high-voltage operation capability, scalability, and LILT and HIHT operation capability (LILT—low intensity low temperature; HIHT—high intensity high temperature).

*This work was done by Brian Spence, Steve White, Kevin Schmid, and Mark Douglas of Deployable Space Systems, Inc. for Glenn Research Center. Further information is contained in a TSP (see page 1).*

*Inquiries concerning rights for the commercial use of this invention should be addressed to NASA Glenn Research Center, Innovative Partnerships Office, Attn: Steven Fedor, Mail Stop 4-8, 21000 Brookpark Road, Cleveland, Ohio 44135. Refer to LEW-18833/4/5-1.*





## **An Integrated, Layered-Spinel Composite Cathode for Energy Storage Applications**

**The composite cathode can be used in rechargeable Li-ion batteries in hybrid electric vehicles, laptops, medical devices, and military vehicles.**

*John H. Glenn Research Center, Cleveland, Ohio*

At low operating temperatures, commercially available electrode materials for lithium-ion batteries do not fully meet the energy and power requirements for NASA's exploration activities. The composite cathode under development is projected to provide the required energy and power densities at low temperatures and its usage will considerably reduce the overall volume and weight of the battery pack.

The newly developed composite electrode material can provide superior electrochemical performance relative to a commercially available lithium cobalt system. One advantage of using a composite cathode is its higher energy density, which can lead to smaller and lighter battery packs. In the current program, different series of layered-spinel composite materials with at least two different systems in an integrated structure were synthesized, and the volumetric and gravimetric energy densities were evaluated. In an integrated network of a

composite electrode, the effect of the combined structures is to enhance the capacity and power capabilities of the material to levels greater than what is possible in current state-of-the-art cathode systems.

The main objective of the current program is to implement a novel cathode material that meets NASA's low temperature energy density requirements. An important feature of the composite cathode is that it has at least two components (e.g., layered and spinel) that are structurally integrated. The layered material by itself is electrochemically inactive; however, upon structural integration with a spinel material, the layered material can be electrochemically activated, thereby delivering a large amount of energy with stable cycling. A key aspect of the innovation has been the development of a scalable process to produce submicron- and micron-scale particles of these composite materials.

An additional advantage of using such a composite electrode material is its low irreversible loss ( $\approx 5\%$ ), which is primarily due to the unique activation of the composite. High columbic efficiency ( $>99\%$ ) upon cycling may indicate the formation of a stable SEI (solid-electrolyte interface) layer, which can contribute to long cycle life. The innovation in the current program, when further developed, will enable the system to maintain high energy and power densities at low temperatures, improve efficiency, and further stabilize and enhance the safety of the cell.

*This work was done by Nader Hagh and Ganesh Skandan of NEI Corporation for Glenn Research Center. Further information is contained in a TSP (see page 1).*

*Inquiries concerning rights for the commercial use of this invention should be addressed to NASA Glenn Research Center, Innovative Partnerships Office, Attn: Steven Fedor, Mail Stop 4-8, 21000 Brookpark Road, Cleveland, Ohio 44135. Refer to LEW-18870-1.*

## **Engineered Multifunctional Surfaces for Fluid Handling**

**These processes create antibacterial and hydrophilic properties on metallic and polymeric surfaces.**

*Lyndon B. Johnson Space Center, Houston, Texas*

Designs incorporating variations in capillary geometry and hydrophilic and/or antibacterial surface properties have been developed that are capable of passive gas/liquid separation and passive water flow. These designs can incorporate capillary grooves and/or surfaces arranged to create linear and circumferential capillary geometry at the micro and macro scale, radial fin configurations, micro holes and patterns, and combinations of the above.

The antibacterial property of this design inhibits the growth of bacteria or

the development of biofilm. The hydrophilic property reduces the water contact angle with a treated substrate such that water spreads into a thin layer atop the treated surface.

These antibacterial and hydrophilic properties applied to a thermally conductive surface, combined with capillary geometry, create a novel heat exchanger capable of condensing water from a humid, two-phase water and gas flow onto the treated heat exchanger surfaces, and passively separating the condensed water from the gas flow in a reduced gravity application.

The overall process to generate the antibacterial and hydrophilic properties includes multiple steps to generate the two different surface properties, and can be divided into two major steps. Step 1 uses a magnetron-based sputtering technique to implant the silver atoms into the base material. A layer of silver is built up on top of the base material. Completion of this step provides the antibacterial property. Step 2 uses a cold-plasma technique to generate the hydrophilic surface property on top of the silver layer generated in Step 1. Completion of this step provides the hy-

drophilic property in addition to the antibacterial property.

Thermally conductive materials are fabricated and then treated to create the antibacterial and hydrophilic surface properties. The individual parts are assembled to create a condensing heat exchanger with antibacterial and hydrophilic surface properties and capillary geometry, which is capable of passive phase separation in a reduced gravity application.

The plasma processes for creating antibacterial and hydrophilic surface properties are suitable for applications where water is present on an exposed surface for an extended time, such that bacteria or biofilms could form, and where there is a need to manage the water on the sur-

face. The processes are also suitable for applications where only the hydrophilic property is needed. In particular, the processes are applicable to condensing heat exchangers (CHXs), which benefit from the antibacterial properties as well as the hydrophilic properties. Water condensing onto the control surfaces of the CHX will provide the moist conditions necessary for the growth of bacteria and the formation of biofilms. The antibacterial properties of the base layer (silver) will mitigate and prevent the growth of bacteria and formation of biofilms that would otherwise reduce the CHX performance. In addition, the hydrophilic properties reduce the water contact angle and prevent water droplets from bridging between control

surfaces. Overall, the hydrophilic properties reduce the pressure drop across the CHX.

*This work was done by Chris Thomas and Yonghui Ma of Orbital Technologies Corporation, and Mark Weislogel for Johnson Space Center. Further information is contained in a TSP (see page 1).*

*In accordance with Public Law 96-517, the contractor has elected to retain title to this invention. Inquiries concerning rights for its commercial use should be addressed to:*

*Orbital Technologies Corp.  
1212 Fourier Drive  
Madison, WI 53717*

*Refer to MSC-24496-1/502-1, volume and number of this NASA Tech Briefs issue, and the page number.*

## Polyolefin-Based Aerogels

**These aerogels can be used for thermal insulation and radiation shielding in apparel, aircraft, race car insulation, and military and recreation tents.**

*Lyndon B. Johnson Space Center, Houston, Texas*

An organic polybutadiene (PB) rubber-based aerogel insulation material was developed that will provide superior thermal insulation and inherent radiation protection, exhibiting the flexibility, resiliency, toughness, and durability typical of the parent polymer, yet with the low density and superior insulation properties associated with the aerogels. The rubbery behaviors of the PB rubber-based aerogels are able to overcome the weak and brittle nature of conventional inorganic and organic aerogel insulation materials. Additionally, with higher content of hydrogen in their structure, the PB rubber aerogels will also provide inherently better radiation protection than those of inorganic and carbon aerogels. Since PB rubber aerogels also exhibit good hydrophobicity due to their hydrocarbon molecular structure, they will provide better performance reliability and durability as well as simpler, more economic, and environmentally friendly production over the conventional silica or other inorganic-based aerogels, which require chemical treatment to make them hydrophobic.

Inorganic aerogels such as silica aerogels demonstrate many unusual and useful properties. There are several strategies to overcoming the drawbacks associated with the weakness and brittleness of silica aerogels. Development of the flexible fiber-reinforced silica aerogel composite blanket has proven one prom-

ising approach, providing a conveniently fielded form factor that is relatively robust toward handling in industrial environments compared to silica aerogel monoliths. However, the flexible silica aerogel composites still have a brittle, dusty character that may be undesirable, or even intolerable, in certain applications. Although the cross-linked organic aerogels such as resorcinol-formaldehyde (RF), polyisocyanurate, and cellulose aerogels show very high impact strength, they are also very brittle with little elongation (i.e., less rubbery). Also, silica and carbon aerogels are less efficient radiation shielding materials due to their lower content of hydrogen element.

The present invention relates to maleinized polybutadiene (or polybutadiene adducted with maleic anhydride)-based aerogel monoliths and composites, and the methods for preparation. Hereafter, they are collectively referred to as polybutadiene aerogels. Specifically, the polybutadiene aerogels of the present invention are prepared by mixing a maleinized polybutadiene resin, a hardener containing a maleic anhydride reactive group, and a catalyst in a suitable solvent, and maintaining the mixture in a quiescent state for a sufficient period of time to form a polymeric gel. After aging at elevated temperatures for a period of time to provide uniformly stronger wet gels, the microporous maleinized polybu-

tadiene-based aerogel is then obtained by removing interstitial solvent by supercritical drying. The mesoporous maleinized polybutadiene-based aerogels contain an open-pore structure, which provides inherently hydrophobic, flexible, nearly unbreakable, less dusty aerogels with excellent thermal and physical properties. The materials can be used as thermal and acoustic insulation, radiation shielding, and vibration-damping materials.

The organic PB-based rubber aerogels are very flexible, no-dust, and hydrophobic organics that demonstrated the following ranges of typical properties: densities of 0.08 to 0.255 g/cm<sup>3</sup>, shrinkage factor (raerogel/rtarget) = 1.2 to 2.84, and thermal conductivity values of 20.0 to 35.0 mW/m-K.

*This work was done by Je Kyun Lee and George Gould of Aspen Aerogels, Inc. for Johnson Space Center. Further information is contained in a TSP (see page 1).*

*In accordance with Public Law 96-517, the contractor has elected to retain title to this invention. Inquiries concerning rights for its commercial use should be addressed to:*

*Aspen Aerogels, Inc.  
30 Forbes Road, Building B  
Northborough, MA 01532  
Phone No.: (508) 691-1111  
E-mail: info@aerogel.com*

*Refer to MSC-24213-1, volume and number of this NASA Tech Briefs issue, and the page number.*

## Adjusting Permittivity by Blending Varying Ratios of SWNTs

High, intermediate, and low permittivity values can be tailored for specific applications.

Lyndon B. Johnson Space Center, Houston, Texas

A new composite material of single-walled carbon nanotubes (SWNTs) displays radio frequency (0 to 1 GHz) permittivity properties that can be adjusted based upon the nanotube composition. When varying ratios of raw to functionalized SWNTs are blended into the silicone elastomer matrix at a total loading of 0.5 percent by weight, a target real permittivity value can be obtained between 70 and 3. This has particular use for designing materials for microwave lenses, microstrips, filters, resonators, high-strength/low-weight electromagnetic interference (EMI) shielding, antennas, waveguides, and low-loss magneto-dielectric products for applications like radome construction.

High permittivities contain higher ratios of raw SWNTs, while lower permittivity values contain higher ratios of functionalized SWNTs. The functionalized SWNTs contain t-butyl aryl groups that allow for good dispersion in the composite due to favorable interactions between the functional groups and the matrix. The functionalized SWNTs are prepared using diazonium chemistry with raw, HiPco-produced SWNTs and t-butyl aniline. Various ratios of raw functionalized SWNTs totaling 0.5 percent by weight (to the elastomer matrix) composition of

nanotubes (weight does not include the added functional groups) are first dispersed in chloroform via bath sonication. The dispersion is then solvent-blended in chloroform with Part A of the NuSil silicone elastomer R-2625. After the solvent is removed through flowing air, the mixture is dried further in a vacuum oven at 60 °C. Part B of the NuSil silicone elastomer R-2615 (10 percent by weight to Part A) is added to the sample and mixed until an even distribution is achieved. The sample is allowed to evacuate in a vacuum desiccator for approximately one hour to remove any air bubbles that are trapped within it. The sample is then thermally cured at ≈200 °C for approximately two hours. At this point, the sample is ready to be tested for dielectric permittivity measurements.

One limitation in this material occurs when there is a variance in the SWNTs that is produced via the HiPco process. If the tubes vary from batch to batch, it is possible that the electric properties of resulting composites may be affected. This, in turn, could also affect the uniformity of the resulting SWNTs that are functionalized. The best consistency in data trends is observed when the composites are made from the same batch of raw and functionalized SWNTs.

It is expected that, in order for the materials described above to be used in the field of microwave radar devices, other additives and components most likely will be incorporated, depending on the intended application. Some examples may include a magnetic component for magneto-dielectric materials, as well as changing the type of polymer host matrix. In addition, metallic particles could be added (1 to 100 weight percent) to bring up the permeability to ranges that equal the permittivity.

*This work was done by James M. Tour, Jason J. Stephenson, and Amanda Higginbotham of Rice University for Johnson Space Center. For further information, contact the JSC Innovation Partnerships Office at (281) 483-3809.*

*In accordance with Public Law 96-517, the contractor has elected to retain title to this invention. Inquiries concerning rights for its commercial use should be addressed to:*

*Rice University*

*Office of Technology Transfer MS 705*

*P.O. Box 1892*

*Houston, TX 77251-1829*

*Phone No.: (713) 348-6188*

*E-mail: techtran@rice.edu*

*Refer to MSC-24344-1, volume and number of this NASA Tech Briefs issue, and the page number.*





## Gravity-Assist Mechanical Simulator for Outreach

**New simulator is more effective than animation.**

*NASA's Jet Propulsion Laboratory, Pasadena, California*

There is no convenient way to demonstrate mechanically, as an outreach (or inreach) topic, the angular momentum trade-offs and the conservation of angular momentum associated with gravity-assist interplanetary trajectories. The mechanical concepts that underlie gravity assist are often misunderstood or confused, possibly because there is no mechanical analog to it in everyday experience. The Gravity Assist Mechanical Simulator is a hands-on solution to this longstanding technical communications challenge. Users intuitively grasp the concepts, meeting specific educational objectives.

A manually spun wheel with high angular mass and low-friction bearings supplies momentum to an attached spherical neodymium magnet that represents a planet orbiting the Sun. A steel bearing ball following a trajectory across a glass plate above the wheel and magnet undergoes an elastic collision with the revolving magnet, illustrating the gravi-



Figure 1. **Gravity Assist Mechanical Simulator:** Yellow outlines the glass surface that represents the ecliptic plane.

tational elastic collision between spacecraft and planet on a gravity-assist interplanetary trajectory.

Manually supplying the angular momentum for the elastic collision, rather than observing an animation, intuitively conveys the concepts, meeting nine specific educational objectives. Many NASA



Figure 2. **Major Components;** support structure and launcher not shown.

and JPL interplanetary missions are enabled by the gravity-assist technique.

*This work was done by David F. Doody and Victor E. White of Caltech, and Mitch D. Scaff for Art Center College of Design and donated to NASA's Jet Propulsion Laboratory. For more information, contact iaoffice@jpl.nasa.gov. NPO-48001*

## Concept for Hydrogen-Impregnated Nanofiber/Photovoltaic Cargo Stowage System

*Lyndon B. Johnson Space Center, Houston, Texas*

A stowage system was conceived that consists of collapsible, reconfigurable stowage bags, rigid polyethylene or metal inserts, stainless-steel hooks, flexible photovoltaic materials, and webbing curtains that provide power generation, thermal stabilization, impact resistance, work/sleeping surfaces, and radiation protection to spaceflight hardware and crewmembers.

Providing materials to the Lunar surface is costly from both a mass and a volume standpoint. Most of the materials that will be transferred to other planets or celestial bodies will not be returned to the Earth. In developing a plan to reconfigure pressurized logistics modules, it was determined that there was a requirement to be able to utilize the inte-

rior volume of these modules and transform them from "Logistics Modules" to "Storage/Living Quarters."

Logistics-to-living must re-utilize stowage bags and the structures that support them to construct living spaces, partitions, furniture, protective shelters from solar particle events, galactic cosmic radiation, and workspaces. In addition to reusing these logistics items for development of the interior living spaces, these items could also be reused outside the habitable volumes to build berms that protect assets from secondary blast ejecta, to define pathways, to stabilize high traffic areas, to protect against dust contamination, to secure assets to mobility elements, to provide thermal protection,

and to create other types of protective shelters for surface experiments.

Unique features of this innovation include hydrogen-impregnated nanofibers encapsulated in a polyethylene coating that act as radiation shielding, flexible solar collection cells that can be connected together with cells from other bags via the webbing walls to create a solar array, and the ability to reconfigure each bag to satisfy multiple needs.

*This work was done by Kriss J. Kennedy, Larry David Toups, and Robert L. Howard of Johnson Space Center; Alan S. Howe of NASA's Jet Propulsion Laboratory; and Jason Eric Poffenberger of Wyle Laboratories. Further information is contained in a TSP (see page 1). MSC-24624-1*

## ✦ **DROP: Durable Reconnaissance and Observation Platform**

**The platform would advance the ability of a soldier or law enforcement person to look ahead or inside of buildings.**

*NASA's Jet Propulsion Laboratory, Pasadena, California*

Robots have been a valuable tool for providing a remote presence in areas that are either inaccessible or too dangerous for humans. Having a robot with a high degree of adaptability becomes crucial during such events. The adaptability that comes from high mobility and high durability greatly increases the potential uses of a robot in these situations, and therefore greatly increases its usefulness to humans. DROP is a lightweight robot that addresses these challenges with the capability to survive large impacts, carry a usable payload, and traverse a variety of surfaces, including climbing vertical surfaces like wood, stone, and concrete. The platform is crash-proof, allowing it to be deployed in ways including being dropped from an unmanned aerial vehicle or thrown from a large MSL-class (Mars Science Laboratory) rover.

Platforms that have been deployed either on Mars or in Iraq/Afghanistan are large, have limited mobility on non-flat terrain, and lack stealth. Conversely, many research platforms have become so small that the limitations on range, terrain, and payload reduce their utility. At 100 to 300 grams, there is a sweet spot where a useful payload can be carried (2.4-GHz video camera and microphone), a useful range is possible (100 meters), the platform can be stealthy and persistent (by virtue of small size), and the platform is still light enough to be crash-proof and capable of advanced mobility like climbing and perching.

The goal of the DROP project is to create a robot that is lightweight, durable, and capable of climbing a variety of vertical surfaces. The robot is also designed to transition easily from horizontal to vertical travel, and vice versa, as well as having the ability to scamper over very rough or rocky approaches. Shape Deposition Manufacturing (a specialized multi-material fabrication process) and rapid prototyping (3D printing) were used to create a new climbing mechanism and simple body design to meet these specifications.

The climbing mechanism uses microspine hooks for climbing. These hooks are arranged in a completely new manner on DROP that will allow climbing without complex mechanics or con-



**DROP** has the ability to climb vertical surfaces, including porous surfaces like wood, using microspine hooks.

trols. This same mechanism has the additional benefit of increasing the maximum ground speed.

The body of DROP merges elements necessary for vertical climbing with a design that is compliant and impact-resistant. The main sections of the body are radially symmetric and allow impact forces to be absorbed similarly, regardless of the orientation during impact. The body features multi-material construction for the purpose of being both lightweight and durable. The use of impact-dampening materials, such as polymers in the Shore 20A-60A hardness range, serves to reduce the impact forces on the controls, the parts most susceptible to impact failure. The body design is similar to the “two-wheeled-plus-tail.”

DROP achieves its mobility through the use of wheel-like microspine sprockets. Microspines provide a low-mass, zero-power solution to climbing. For these reasons, microspines are desirable for use in smaller robots. Creating a circular array of these microspines, each with an independent flexible suspension, allows continuous engagement with the climbing surface using a

straightforward, rotary motion. The suspension feature enables each microspine hook to engage the surface independently of other hooks, increasing the chances of multiple engagements. The flexibility of the suspension then allows the microspine hook to remain engaged as the sprocket rotates through a greater range of motion than would otherwise be possible.

The body is constructed from a high-elongation, polyamide-based material and features a two-wheeled design with a tail for stability. The body can be produced quickly and cheaply via selective laser sintering (SLS) from materials that feature high impact resistance. The body is divided into two main components: a central section that houses the motors, and a tail section that contains the batteries, RF receiver, and microprocessor unit. The center and tail sections are connected by alternating sections of SLS material and a polymer of Shore-60A hardness. These alternating sections of hard and soft allow the tail to bend and twist relative to the central section. This flexible connection not only allows the two sections to absorb

impacts independently, but also serves to absorb impacts through its capacity to deform.

Two motors allow the robot to turn in confined spaces and climb with a usable payload. A microcontroller makes it possible to accurately manipulate the rotation of the microspine sprockets. Doing so enables DROP to use one motor control algorithm for ground travel at high

speed and another for more controlled, secure climbing.

*This work was done by Aaron Parness and Clifford F. McKenzie of Caltech for NASA's Jet Propulsion Laboratory. Further information is contained in a TSP (see page 1).*

*In accordance with Public Law 96-517, the contractor has elected to retain title to this invention. Inquiries concerning rights for its commercial use should be addressed to:*

*Innovative Technology Assets Management  
JPL*

*Mail Stop 202-233*

*4800 Oak Grove Drive*

*Pasadena, CA 91109-8099*

*E-mail: [iaoffice@jpl.nasa.gov](mailto:iaoffice@jpl.nasa.gov)*

*Refer to NPO-48314, volume and number of this NASA Tech Briefs issue, and the page number.*





### **Developing Physiologic Models for Emergency Medical Procedures Under Microgravity**

*Lyndon B. Johnson Space Center, Houston, Texas*

Several technological enhancements have been made to METI's commercial Emergency Care Simulator (ECS) with regard to how microgravity affects human physiology. The ECS uses both a software-only lung simulation, and an integrated mannequin lung that uses a physical lung bag for creating chest excursions, and a digital simulation of lung mechanics and gas exchange. METI's patient simulators incorporate models

of human physiology that simulate lung and chest wall mechanics, as well as pulmonary gas exchange.

Microgravity affects how O<sub>2</sub> and CO<sub>2</sub> are exchanged in the lungs. Procedures were also developed to take into affect the Glasgow Coma Scale for determining levels of consciousness by varying the ECS eye-blinking function to partially indicate the level of consciousness of the patient. In addition, the ECS was modi-

fied to provide various levels of pulses from weak and thready to hyper-dynamic to assist in assessing patient conditions from the femoral, carotid, brachial, and pedal pulse locations.

*This work was done by Nigel Parker and Veronica O'Quinn of Medical Education Tech, Inc. for Johnson Space Center. Further information is contained in a TSP (see page 1). MSC-23922-1*





## Spectroscopic Chemical Analysis Methods and Apparatus

Ames Research Center, Moffett Field, California

This invention relates to non-contact spectroscopic methods and apparatus for performing chemical analysis and the ideal wavelengths and sources needed for this analysis. It employs deep ultraviolet (200- to 300-nm spectral range) electron-beam-pumped wide bandgap semiconductor lasers, incoherent wide bandgap semiconductor light-emitting devices, and hollow cathode metal ion lasers.

Three achieved goals for this innovation are to reduce the size (under 20 L), reduce the weight [under 100 lb ( $\approx 45$  kg)], and reduce the power consumption (under 100 W). This method can be used in microscope or macroscope to provide measurement of Raman and/or native fluorescence emission spectra either by point-by-point measurement, or by global

imaging of emissions within specific ultraviolet spectral bands. In other embodiments, the method can be used in analytical instruments such as capillary electrophoresis, capillary electrochromatography, high-performance liquid chromatography, flow cytometry, and related instruments for detection and identification of unknown analytes using a combination of native fluorescence and/or Raman spectroscopic methods.

This design provides an electron-beam-pumped semiconductor radiation-producing method, or source, that can emit at a wavelength (or wavelengths) below 300 nm, e.g. in the deep ultraviolet between about 200 and 300 nm, and more preferably less than 260 nm. In some variations, the method is to produce incoherent radiation, while in other implementa-

tions it produces laser radiation. In some variations, this object is achieved by using an AlGaN emission medium, while in other implementations a diamond emission medium may be used.

This instrument irradiates a sample with deep UV radiation, and then uses an improved filter for separating wavelengths to be detected. This provides a multi-stage analysis of the sample. To avoid the difficulties related to producing deep UV semiconductor sources, a pumping approach has been developed that uses ballistic electron beam injection directly into the active region of a wide bandgap semiconductor material.

*This work was done by William F. Hug and Ray D. Reid of Photon Systems, Inc. for Ames Research Center. Further information is contained in a TSP (see page 1). ARC-15298-1*

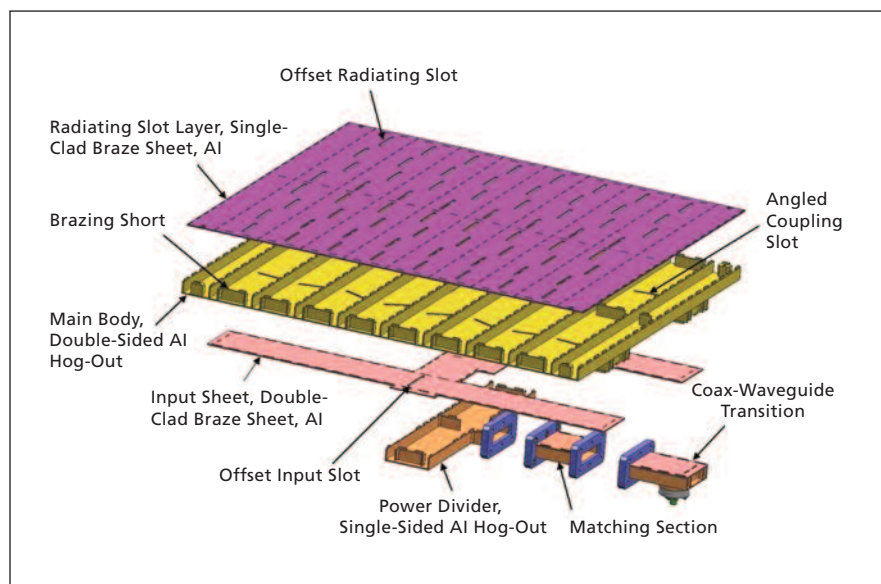
## Low Average Sidelobe Slot Array Antennas for Radiometer Applications

Slot arrays are used in radar, remote sensing, and communications applications.

NASA's Jet Propulsion Laboratory, Pasadena, California

In radiometer applications, it is required to design antennas that meet low average sidelobe levels and low average return loss over a specified frequency bandwidth. It is a challenge to meet such specifications over a frequency range when one uses resonant elements such as waveguide feed slots. In addition to their inherent narrow frequency band performance, the problem is exacerbated due to modeling errors and manufacturing tolerances. There was a need to develop a design methodology to solve the problem.

An iterative design procedure was developed by starting with an array architecture, lattice spacing, aperture distribution, waveguide dimensions, etc. The array was designed using Elliott's technique with appropriate values of the total slot conductance in each radiating waveguide, and the total resistance in each feed waveguide. Subsequently, the



The **Slot Array Architecture** consists of four machined mechanical layers forming three electrical layers as shown in the figure.

array performance was analyzed by the full wave method of moments solution to the pertinent integral equations. Monte Carlo simulations were also carried out to account for amplitude and phase errors introduced for the aperture distribution due to modeling errors as well as manufacturing tolerances. If the design margins for the average sidelobe level and the average return loss were not adequate, array architecture, lattice spacing, aperture distribution, and waveguide dimensions were varied in subsequent iterations.

Once the design margins were found to be adequate, the iteration was stopped and a good design was achieved. A symmetric array architecture was found to meet the design specification with adequate margin.

The specifications were near  $-40$  dB for angular regions beyond 30 degrees from broadside. Separable Taylor distribution with  $n_{bar}=4$  and  $-35$  dB sidelobe specification was chosen for each principal plane. A non-separable distribution obtained by the genetic algorithm was found to have similar characteristics.

The element spacing was obtained to provide the required beamwidth and close to a null in the E-plane end-fire direction. Because of the alternating slot offsets, grating lobes called butterfly lobes are produced in non-principal planes close to the H-plane. An attempt to reduce the influence of such grating lobes resulted in a symmetric design.

*This work was done by Sembiam Rengaranjan, Mark S. Zawadzki, and Richard E. Hodges of Caltech for NASA's Jet Propulsion Laboratory. For more information, contact iaoffice@jpl.nasa.gov. NPO-48481*

---

## Motion-Corrected 3D Sonic Anemometer for Tethersondes and Other Moving Platforms

*Goddard Space Flight Center, Greenbelt, Maryland*

To date, it has not been possible to apply 3D sonic anemometers on tether-sondes or similar atmospheric research platforms due to the motion of the supporting platform. A tether-sonde module including both a 3D sonic anemometer and associated motion correction sensors has been developed, enabling motion-corrected 3D winds to be measured from a moving platform such as a tether-sonde.

Blimps and other similar lifting systems are used to support tether-sondes — meteorological devices that fly on the tether of a blimp or similar platform. To date, tether-sondes have been limited to making basic meteorological measurements (pressure, temperature, humidity, and wind speed and direction). The motion of the tether-sonde has precluded

the addition of 3D sonic anemometers, which can be used for high-speed flux measurements, thereby limiting what has been achieved to date with tether-sondes. The tether-sonde modules fly on a tether that can be constantly moving and swaying. This would introduce enormous error into the output of an uncorrected 3D sonic anemometer. The motion correction that is required must be implemented in a low-weight, low-cost manner to be suitable for this application. Until now, flux measurements using 3D sonic anemometers could only be made if the 3D sonic anemometer was located on a rigid, fixed platform such as a tower. This limited the areas in which they could be set up and used.

The purpose of the innovation was to enable precise 3D wind and flux meas-

urements to be made using tether-sondes. In brief, a 3D accelerometer and a 3D gyroscope were added to a tether-sonde module along with a 3D sonic anemometer. This combination allowed for the necessary package motions to be measured, which were then mathematically combined with the measured winds to yield motion-corrected 3D winds.

At the time of this reporting, no tether-sonde has been able to make any wind measurement other than a basic wind speed and direction measurement. The addition of a 3D sonic anemometer is unique, as is the addition of the motion-correction sensors.

*This work was done by John Bognar of Anasphere, Inc. for Goddard Space Flight Center. Further information is contained in a TSP (see page 1). GSC-16310-1*

---

## Water Treatment Systems for Long Spaceflights

**These methods enable recycling of urine to provide drinking water on long spaceflights.**

*Ames Research Center, Moffett Field, California*

Space exploration will require new life support systems to support the crew on journeys lasting from a few days to several weeks, or longer. These systems should also be designed to reduce the mass required to keep humans alive in space. Water accounts for about 80 percent of the daily mass intake required to keep a person alive. As a result, recycling water offers a high return on investment for space life support. Water recycling can also increase mission safety by pro-

viding an emergency supply of drinking water, where another supply is exhausted or contaminated.

These technologies also increase safety by providing a lightweight backup to stored supplies, and they allow astronauts to meet daily drinking water requirements by recycling the water contained in their own urine. They also convert urine into concentrated brine that is biologically stable and non-threatening, and can be safely stored

onboard. This approach eliminates the need to have a dedicated vent to dump urine overboard.

These needs are met by a system that provides a contaminant treatment pouch, referred to as a “urine cell” or “contaminant cell,” that converts urine or another liquid containing contaminants into a fortified drink, engineered to meet human hydration, electrolyte, and caloric requirements, using a variant of forward osmosis (FO) to draw

water from a urine container into the concentrated fortified drink as part of a recycling stage. An activated carbon pretreatment removes most organic molecules. Salinity of the initial liquid mix (urine plus other) is synergistically used to enhance the precipitation of organic molecules so that activated carbon can remove most of the organics. A functional osmotic bag is then used to remove inorganic contaminants. If a contaminant is processed for which the saline content is different than optimal for precipitating organic molecules, the saline content of the liquid should be adjusted toward the optimal value for that contaminant.

A first urine treatment method converts urine into a fortified sports drink,

resembling Gatorade, using a first urine cell. A membrane filter that is hydrophilic allows water to diffuse through the filter but blocks most contaminants using a micropore construction. Water is drawn through the membrane by a forward osmotic pressure differential, generated by the liquid feed, sugars, and electrolytes contained in a concentrated sports drink, which is positioned on the product (output) side of the membrane. Water, initially contained in urine, diffuses through the membrane to approximately balance the concentration gradient. As a result, the sports drink will become diluted and the urine will become concentrated. The maximum number of urine recycling sessions is about ten. The process is a modification of a

process used in a water treatment cell from Hydration Technologies X-Pack.

A second urine treatment method uses osmotic distillation and a hydrophobic, microporous membrane filter, with a product (output) side exposed to a second liquid phase that is capable of absorbing wastewater that is presented on the input side of the filter. The method is sometimes referred to as isothermal membrane distillation and is driven by a vapor pressure gradient rather than by a temperature gradient.

*This work was done by Michael T. Flynn of Ames Research Center and Sherwin J. Gormly of the National Space Grant Foundation. Further information is contained in a TSP (see page 1). ARC-15890-1*

---

## **Microchip Non-Aqueous Capillary Electrophoresis ( $\mu$ NACE) Method to Analyze Long-Chain Primary Amines**

*NASA's Jet Propulsion Laboratory, Pasadena, California*

A protocol was developed as a first step in analyzing the complex organic aerosols present on Saturn's moon Titan, as well as the analogues of these aerosols (tholins) made on Earth. Labeling of primary amines using Pacific Blue™ succinimidyl ester is effected in ethanol with 25 mM triethylamine to maintain basic conditions. This reaction is allowed to equilibrate for at least one hour. Separation of the labeled primary amines is performed in ethanol with 1.05 M acetic acid, and 50 mM ammonium acetate in a commercial two-layer glass device with a standard cross-microchannel measuring 50 microns wide by 20 microns deep. Injection po-

tentials are optimized at 2 kV from the sample (negative) to the waste well (positive), with slight bias applied to the other two wells (-0.4 and -0.8 V) to pinch the injection plug for the 30-s injection. Separation is performed at a potential of 5 kV along the channel, which has an effective separation distance of 7 cm.

The use of ethanol in this method means that long-chain primary amines can be dissolved. Due to the low pH of the separation buffer, electro-osmotic flow (EOF) is minimized to allow for separation of both short-chain and long-chain amines. As the freezing point of ethanol is much lower than water, this

protocol can perform separations at temperatures lower than 0 °C, which would not be possible in aqueous phase. This is of particular importance when considering *in situ* sampling of Titan aerosols, where unnecessary heating of the sample (even to room temperature) would lead to decomposition or unpredictable side reactions, which would make it difficult to characterize the sample appropriately.

*This work was done by Peter A. Willis and Maria Mora of Caltech, and Morgan L. Cable and Amanda M. Stockton of ORAU for NASA's Jet Propulsion Laboratory. For more information, contact [iaoffice@jpl.nasa.gov](mailto:iaoffice@jpl.nasa.gov). NPO-48615*

---

## **Low-Cost Phased Array Antenna for Sounding Rockets, Missiles, and Expendable Launch Vehicles**

**Commercial applications include conformal satellite antennas for recreational vehicles, cars, and residences.**

*Goddard Space Flight Center, Greenbelt, Maryland*

A low-cost beamformer phased array antenna has been developed for expendable launch vehicles, rockets, and missiles. It utilizes a conformal array antenna of ring or individual radiators (design varies depending on application) that is designed to be fed by the recently

developed hybrid electrical/mechanical (vendor-supplied) phased array beamformer. The combination of these new array antennas and the hybrid beamformer results in a conformal phased array antenna that has significantly higher gain than traditional "omni" an-

tennas, and costs an order of magnitude or more less than traditional phased array designs.

Existing omnidirectional antennas for sounding rockets, missiles, and expendable launch vehicles (ELVs) do not have sufficient gain to support the required

communication data rates via the space network. Missiles and smaller ELVs are often stabilized in flight by a fast (i.e. 4 Hz) roll rate. This fast roll rate, combined with vehicle attitude changes, greatly increases the complexity of the high-gain antenna beam-tracking problem. Phased arrays for larger ELVs with roll control are prohibitively expensive. Prior techniques involved a traditional fully electronic phased array solution, combined with highly complex and very fast inertial measurement unit phased array beamformers.

The functional operation of this phased array is substantially different from traditional phased arrays in that it uses a hybrid electrical/mechanical

beamformer that creates the relative time delays for steering the antenna beam via a small physical movement of variable delay lines. This movement is controlled via an innovative antenna control unit that accesses an internal measurement unit for vehicle attitude information, computes a beam-pointing angle to the target, then points the beam via a stepper motor controller. The stepper motor on the beamformer controls the beamformer variable delay lines that apply the appropriate time delays to the individual array elements to properly steer the beam.

The array of phased ring radiators is unique in that it provides improved gain

for a small rocket or missile that uses spin stabilization for stability. The antenna pattern created is symmetric about the roll axis (like an omnidirectional wrap-around), and is thus capable of providing continuous coverage that is compatible with very fast spinning rockets. For larger ELVs with roll control, a linear array of elements can be used for the 1D scanned beamformer and phased array, or a 2D scanned beamformer can be used with an  $N \times N$  element array.

*This work was done by Daniel Mullinix, Kenneth Hall, Bruce Smith, and Brian Corbin of Goddard Space Flight Center. Further information is contained in a TSP (see page 1). GSC-15805-1*

---

## Mars Science Laboratory Engineering Cameras

*NASA's Jet Propulsion Laboratory, Pasadena, California*

NASA's Mars Science Laboratory (MSL) Rover, which launched to Mars in 2011, is equipped with a set of 12 engineering cameras. These cameras are build-to-print copies of the Mars Exploration Rover (MER) cameras, which were sent to Mars in 2003. The engineering cameras weigh <300 grams each and use <3 W of power. Images returned from the engineering cameras are used to navigate the rover on the Martian surface, deploy the rover robotic arm, and ingest samples into the rover sample processing system. The navigation cam-

eras (Navcams) are mounted to a pan/tilt mast and have a 45-degree square field of view (FOV) with a pixel scale of 0.82 mrad/pixel.

The hazard avoidance cameras (Hazcams) are body-mounted to the rover chassis in the front and rear of the vehicle and have a 124-degree square FOV with a pixel scale of 2.1 mrad/pixel. All of the cameras utilize a frame-transfer CCD (charge-coupled device) with a 1024x1024 imaging region and red/near IR bandpass filters centered at 650 nm. The MSL engi-

neering cameras are grouped into two sets of six: one set of cameras is connected to rover computer "A" and the other set is connected to rover computer "B". The MSL rover carries 8 Hazcams and 4 Navcams.

*This work was done by Justin N. Maki, David L. Thiessen, Ali M. Pourangi, Peter A. Kobzeff, Steven W. Lee, Arsham Dingizian, and Mark A. Schwochert of Caltech for NASA's Jet Propulsion Laboratory. For more information, contact [iaoffice@jpl.nasa.gov](mailto:iaoffice@jpl.nasa.gov). NPO-48550*

---

## Seismic Imager Space Telescope

**The imager will offer alternative ways of studying earthquakes and improve early warning systems.**

*NASA's Jet Propulsion Laboratory, Pasadena, California*

A concept has been developed for a geostationary seismic imager (GSI), a space telescope in geostationary orbit above the Pacific coast of the Americas that would provide movies of many large earthquakes occurring in the area from Southern Chile to Southern Alaska. The GSI movies would cover a field of view as long as 300 km, at a spatial resolution of 3 to 15 m and a temporal resolution of 1 to 2 Hz, which is sufficient for accurate measurement of surface displacements and photometric changes induced by seismic waves. Computer processing of the movie images

would exploit these dynamic changes to accurately measure the rapidly evolving surface waves and surface ruptures as they happen. These measurements would provide key information to advance the understanding of the mechanisms governing earthquake ruptures, and the propagation and arrest of damaging seismic waves.

GSI operational strategy is to react to earthquakes detected by ground seismometers, slewing the satellite to point at the epicenters of earthquakes above a certain magnitude. Some of these earthquakes will be foreshocks of larger earth-

quakes; these will be observed, as the spacecraft would have been pointed in the right direction. This strategy was tested against the historical record for the Pacific coast of the Americas, from 1973 until the present. Based on the seismicity recorded during this time period, a GSI mission with a lifetime of 10 years could have been in position to observe at least 13 (22 on average) earthquakes of magnitude larger than 6, and at least one (2 on average) earthquake of magnitude larger than 7.

A GSI would provide data unprecedented in its extent and temporal and

spatial resolution. It would provide this data for some of the world's most seismically active regions, and do so better and at a lower cost than could be done with ground-based instrumentation. A GSI would revolutionize the understanding of earthquake dynamics, perhaps leading ultimately to effective warning capabilities, to improved management of earthquake risk, and to improved public safety policies.

The position of the spacecraft, its high optical quality, large field of view, and large field of regard will make it an ideal platform for other scientific studies. The same data could be simply reused for other studies. If different data, such as multi-spectral data, is required, additional instruments could share the telescope.

*This work was done by Erkin Sidick, Keith Coste, Thomas J. Cunningham, Michael W.*

*Sievers, Gregory S. Agnes, Otto R. Polanco, Joseph J. Green, Bruce A. Cameron, David C. Redding, Jean Philippe Avouac, Jean Paul Ampuero, and Sebastien Leprince of Caltech; Rémi Michel of the Université Pierre et Marie Curie; and Jesse Redding of UC Berkeley for NASA's Jet Propulsion Laboratory. Further information is contained in a TSP (see page 1). NPO-48469*





## Estimating Sea Surface Salinity and Wind Using Combined Passive and Active L-Band Microwave Observations

NASA's Jet Propulsion Laboratory, Pasadena, California

Several L-band microwave radiometer and radar missions have been, or will be, operating in space for land and ocean observations. These include the NASA Aquarius mission and the Soil Moisture Active Passive (SMAP) mission, both of which use combined passive/active L-band instruments. Aquarius's passive/active L-band microwave sensor has been designed to map the salinity field at the surface of the ocean from space. SMAP's primary objectives are for soil moisture and freeze/thaw detection, but it will operate continuously over the ocean, and hence will have significant potential for ocean surface research.

In this innovation, an algorithm has been developed to retrieve simultaneously ocean surface salinity and wind from combined passive/active L-band microwave observations of sea surfaces. The algorithm takes advantage of the differ-

ing response of brightness temperatures and radar backscatter to salinity, wind speed, and direction, thus minimizing the least squares error (LSE) measure, which signifies the difference between measurements and model functions of brightness temperatures and radar backscatter. The algorithm uses the conjugate gradient method to search for the local minima of the LSE.

Three LSE measures with different measurement combinations have been tested. The first LSE measure uses passive microwave data only with retrieval errors reaching 1 to 2 psu (practical salinity units) for salinity, and 1 to 2 m/s for wind speed. The second LSE measure uses both passive and active microwave data for vertical and horizontal polarizations. The addition of active microwave data significantly improves the retrieval accuracy by about a factor of five. To mitigate the impact of Faraday

rotation on satellite observations, the third LSE measure uses measurement combinations invariant under the Faraday rotation. For Aquarius, the expected RMS SSS (sea surface salinity) error will be less than about 0.2 psu for low winds, and increases to 0.3 psu at 25 m/s wind speed for warm waters (25 °C).

To achieve the required 0.2 psu accuracy, the impact of sea surface roughness (e.g. wind-generated ripples) on the observed brightness temperature has to be corrected to better than one tenth of a degree Kelvin. With this algorithm, the accuracy of retrieved wind speed will be high, varying from a few tenths to 0.6 m/s. The expected direction accuracy is also excellent (<10°) for mid to high winds, but degrades for lower speeds (<7 m/s).

*This work was done by Simon H. Yueh and Mario J. Chabell of Caltech for NASA's Jet Propulsion Laboratory. For more information, contact [iaoffice@jpl.nasa.gov](mailto:iaoffice@jpl.nasa.gov). NPO-48097*

## A Posteriori Study of a DNS Database Describing Supercritical Binary-Species Mixing

Resulting flow models can be used in automotive, aircraft engine, and chemical engineering applications.

NASA's Jet Propulsion Laboratory, Pasadena, California

Currently, the modeling of supercritical-pressure flows through Large Eddy Simulation (LES) uses models derived for atmospheric-pressure flows. Those atmospheric-pressure flows do not exhibit the particularities of high density-gradient magnitude features observed both in experiments and simulations of supercritical-pressure flows in the case of two species mixing. To assess whether the current LES modeling is appropriate and if found not appropriate to propose higher-fidelity models, a LES *a posteriori* study has been conducted for a mixing layer that initially contains different species in the lower and upper streams, and where the initial pressure is larger than the critical pressure of either

species. An initially-imposed vorticity perturbation promotes roll-up and a double pairing of four initial span-wise vortices into an ultimate vortex that reaches a transitional state.

The LES equations consist of the differential conservation equations coupled with a real-gas equation of state, and the equation set uses transport properties depending on the thermodynamic variables. Unlike all LES models to date, the differential equations contain, additional to the subgrid scale (SGS) fluxes, a new SGS term that is a pressure correction in the momentum equation. This additional term results from filtering of Direct Numerical Simulation (DNS) equations, and repre-

sents the gradient of the difference between the filtered pressure and the pressure computed from the filtered flow field.

A previous *a priori* analysis, using a DNS database for the same configuration, found this term to be of leading order in the momentum equation, a fact traced to the existence of high-density-gradient magnitude regions that populated the entire flow; in the study, models were proposed for the SGS fluxes as well as this new term. In the present study, the previously proposed constant-coefficient SGS-flux models of the *a priori* investigation are tested *a posteriori* in LES, devoid of or including, the SGS pressure correction term. The present

pressure-correction model is different from, and more accurate as well as less computationally intensive than that of the *a priori* study.

The constant-coefficient SGS-flux models encompass the Smagorinsky (SMC), in conjunction with the Yoshizawa (YO) model for the trace, the Gradient (GRC) and the Scale Similarity (SSC) models, all exercised with the *a priori* study constant coefficients calibrated at the transitional state. The LES

comparison is performed with the filtered-and-coarsened (FC) DNS, which represents an ideal LES solution. Expectably, an LES model devoid of SGS terms is shown to be considerably inferior to models containing SGS effects. Among models containing SGS effects, those including the pressure-correction term are substantially superior to those devoid of it. The sensitivity of the predictions to the initial conditions and grid size are also investigated.

Thus, it has been discovered that, additional to the atmospheric-pressure models currently used, a new model is necessary to simulate supercritical-pressure flows. This model depends on the thermodynamic characteristics of the chemical species involved.

*This work was done by Josette Bellan and Ezgi Taskinoglu of Caltech for NASA's Jet Propulsion Laboratory. For more information, contact iaoffice@jpl.nasa.gov. NPO-46733*

---

## Scalable SCPPM Decoder

*NASA's Jet Propulsion Laboratory, Pasadena, California*

A decoder was developed that decodes a serial concatenated pulse position modulation (SCPPM) encoded information sequence. The decoder takes as input a sequence of four bit log-likelihood ratios (LLR) for each PPM slot in a codeword via a XAUI 10-Gb/s quad optical fiber interface. If the decoder is unavailable, it passes the LLRs on to the next decoder via a XAUI 10-Gb/s quad optical fiber interface. Otherwise, it decodes the se-

quence and outputs information bits through a 1-GB/s Ethernet UDP/IP (User Datagram Protocol/Internet Protocol) interface.

The throughput for a single decoder unit is 150-Mb/s at an average of four decoding iterations; by connecting a number of decoder units in series, a decoding rate equal to that of the aggregate rate is achieved. The unit is controlled through a 1-GB/s Ethernet UDP/IP interface.

This ground station decoder was developed to demonstrate a deep space optical communication link capability, and is unique in the scalable design to achieve real-time SCPPM decoding at the aggregate data rate.

*This work was done by Kevin J. Quirk, Jonathan W. Gin, Danh H. Nguyen, Huy Nguyen, Michael A. Nakashima, and Bruce E. Moision of Caltech for NASA's Jet Propulsion Laboratory. For more information, contact iaoffice@jpl.nasa.gov. NPO-47729*



## 🌀 QuakeSim 2.0

QuakeSim 2.0 improves understanding of earthquake processes by providing modeling tools and integrating model applications and various heterogeneous data sources within a Web services environment. QuakeSim is a multi-source, synergistic, data-intensive environment for modeling the behavior of earthquake faults individually, and as part of complex interacting systems. Remotely sensed geodetic data products may be explored, compared with faults and landscape features, mined by pattern analysis applications, and integrated with models and pattern analysis applications in a rich Web-based and visualization environment. Integration of heterogeneous data products with pattern informatics tools enables efficient development of models.

Federated database components and visualization tools allow rapid exploration of large datasets, while pattern informatics enables identification of subtle, but important, features in large data sets. QuakeSim is valuable for earthquake investigations and modeling in its current state, and also serves as a prototype and nucleus for broader systems under development.

The framework provides access to physics-based simulation tools that model the earthquake cycle and related crustal deformation. Spaceborne GPS and Interferometric Synthetic Aperture (InSAR) data provide information on near-term crustal deformation, while paleoseismic geologic data provide longer-term information on earthquake fault processes. These data sources are integrated into QuakeSim's QuakeTables database system, and are accessible by users or various model applications. UAVSAR repeat pass interferometry data products are added to the QuakeTables database, and are available through a browseable map interface or Representational State Transfer (REST) interfaces. Model applications can retrieve data from QuakeTables, or from third-party GPS velocity data services; alternatively, users can manually input parameters into the models.

Pattern analysis of GPS and seismicity data has proved useful for mid-term forecasting of earthquakes, and for detecting subtle changes in crustal deformation. The GPS time series analysis has

also proved useful as a data-quality tool, enabling the discovery of station anomalies and data processing and distribution errors. Improved visualization tools enable more efficient data exploration and understanding. Tools provide flexibility to science users for exploring data in new ways through download links, but also facilitate standard, intuitive, and routine uses for science users and end users such as emergency responders.

*This work was done by Andrea Donnellan, Jay W. Parker, Gregory A. Lyzenga, Robert A. Granat, and Charles D. Norton of Caltech; John B. Rundle of University of California, Davis; Marlon E. Pierce and Geoffrey C. Fox of Indiana University; Dennis Mcleod of University of Southern California; and Lisa Grant Ludwig of University of California, Irvine for NASA's Jet Propulsion Laboratory. For more information, access <http://quakesim.org>.*

*This software is available for commercial licensing. Please contact Daniel Broderick of the California Institute of Technology at [danielb@caltech.edu](mailto:danielb@caltech.edu). Refer to NPO-48579.*

## 🌀 HURON (HUMAN and Robotic Optimization Network) Multi-Agent Temporal Activity Planner/Scheduler

HURON solves the problem of how to optimize a plan and schedule for assigning multiple agents to a temporal sequence of actions (e.g., science tasks). Developed as a generic planning and scheduling tool, HURON has been used to optimize space mission surface operations. The tool has also been used to analyze lunar architectures for a variety of surface operational scenarios in order to maximize return on investment and productivity. These scenarios include numerous science activities performed by a diverse set of agents: humans, teleoperated rovers, and autonomous rovers. Once given a set of agents, activities, resources, resource constraints, temporal constraints, and dependencies, HURON computes an optimal schedule that meets a specified goal (e.g., maximum productivity or minimum time), subject to the constraints.

HURON performs planning and scheduling optimization as a graph search in state-space with forward progression. Each node in the graph con-

tains a state "instance." Starting with the initial node, a graph is automatically constructed with new successive nodes of each new state to explore. The optimization uses a set of pre-conditions and post-conditions to create the children states.

The Python language was adopted to not only enable more agile development, but to also allow the domain experts to easily define their optimization models. A graphical user interface was also developed to facilitate real-time search information feedback and interaction by the operator in the search optimization process.

The HURON package has many potential uses in the fields of Operations Research and Management Science where this technology applies to many commercial domains requiring optimization to reduce costs. For example, optimizing a fleet of transportation truck routes, aircraft flight scheduling, and other route-planning scenarios involving multiple agent task optimization would all benefit by using HURON.

*This work was done by Hook Hua, Joseph J. Mrozinski, Alberto Elfes, Virgil Adumitroaie, Kacie E. Shelton, Jeffrey H. Smith, William P. Lincoln, and Charles R. Weisbin of Caltech for NASA's Jet Propulsion Laboratory. For more information, contact [iaoffice@jpl.nasa.gov](mailto:iaoffice@jpl.nasa.gov).*

*This software is available for commercial licensing. Please contact Daniel Broderick of the California Institute of Technology at [danielb@caltech.edu](mailto:danielb@caltech.edu). Refer to NPO-47573.*

## 🌀 MPST Software: MoonKommand

This software automatically processes Sally Ride Science (SRS) delivered MoonKAM camera control files (ccf) into uplink products for the GRAIL-A and GRAIL-B spacecraft as part of an education and public outreach (EPO) extension to the Grail Mission. Once properly validated and deemed safe for execution onboard the spacecraft, MoonKommand generates the command products via the Automated Sequence Processor (ASP) and generates uplink (.scmf) files for radiation to the Grail-A and/or Grail-B spacecraft. Any errors detected along the way are reported back to SRS via email. With MoonKommand, SRS can control their

EPO instrument as part of a fully automated process.

Inputs are received from SRS as either image capture files (.ccfcd) for new image requests, or downlink/delete files (.ccfdl) for requesting image downlink from the instrument and on-board memory management. The MoonKommand outputs are command and file-load (.scmf) files that will be up-

linked by the Deep Space Network (DSN). Without MoonKommand software, uplink product generation for the MoonKAM instrument would be a manual process.

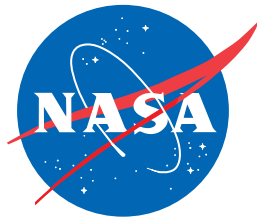
The software is specific to the MoonKAM instrument on the GRAIL mission. At the time of this writing, the GRAIL mission was making final preparations to begin the science phase, which was

scheduled to continue until June 2012.

*This work was done by John H. Kwok, Jared A. Call, Teerapat Khanapornphan, and Joseph S. Stehly of Caltech for NASA's Jet Propulsion Laboratory. For more information, contact iaoffice@jpl.nasa.gov.*

*This software is available for commercial licensing. Please contact Daniel Broderick of the California Institute of Technology at danielb@caltech.edu. Refer to NPO-47693.*





National Aeronautics and  
Space Administration